Journal of Power Sources 196 (2011) 7812–7815

Contents lists available at ScienceDirect

Journal of Power Sources

journal homepage: www.elsevier.com/locate/jpowsour

Short communication

Equivalent circuit components of nickel–metal hydride battery at different states of charge

K.H. Norian*

Electrical and Computer Engineering Department, 19 Memorial Drive West, Lehigh University, Bethlehem, PA 18015, USA

ARTICLE INFO

Article history:
Received 8 March 2011
Received in revised form 31 March 2011
Accepted 1 April 2011
Available online 27 April 2011

Keywords:
Nickel–metal hydride battery
State of charge
Battery equivalent circuit

ABSTRACT

Equations that describe the voltage variations with time of rechargeable batteries during charging and discharging were used to determine the component values of the equivalent circuit of nickel–metal hydride batteries under different states of charge (SOC). The equivalent circuit of the battery was described as an ideal voltage source in series with a resistor and the parallel combination of a resistor and a capacitor. The battery model used different values of resistance and capacitance, in the parallel combination, during the different phases of the discharge–rest–charge–rest sequence. The results show that the resistances in the equivalent circuit are approximately constant with variations in the SOC. For the discharge and charge phases the capacitor value increased and decreased, respectively, as the SOC decreased. The value of the capacitor in the parallel *RC* circuit is an indicator of the battery SOC.

1. Introduction

The engineering design and performance evaluation of battery dependent systems require an electrical equivalent circuit for the battery. The variation of the equivalent circuit components of nickel–metal hydride (NiMH) batteries as a function of the battery state of charge (SOC) is given in this paper. Impedance methods have been used in the past to model the state of charge of batteries [1,2]. Other methods use coulomb counting [3] or the measurement of the open circuit voltage to estimate the SOC [4]. The present work uses a transient method to model the battery parameters at different SOC.

The most basic circuit of the battery is a voltage source in series with the internal resistance. The electrochemical processes of rechargeable batteries [5,6] lead to a second, and more precise, equivalent circuit comprising a voltage source in series with a resistor and a parallel combination of a resistor and a capacitor [7–11]; the voltage–resistance–capacitance (VRC) model. The latter is used to model the battery under conditions of constant state of charge and constant temperature. This model is valid for discharge times of the order of seconds. This model was used in the present work together with a battery measurement method based on transient analysis.

The VRC model was used in the present work in a transient measurement method that uses the discharge–rest–charge–rest sequence of a rechargeable battery with different values for the resistor and capacitor, in the parallel combination of R and C, for the charge and discharge phases and for the intervening rest periods. Equations for the temporal variation of the battery voltage during transients, including boundaries at transitions between transients, were used to calculate the equivalent circuit components for nickel–metal hydride batteries at three values of SOC.

2. Theory

The equivalent circuit of the battery appears to the left of terminals a and b in Fig. 1 where $v(t)$ is the battery voltage. It is a series combination of the open circuit battery voltage V_{oc}, a resistor, and the equivalent of the parallel combination of a resistor and a capacitor.

Fig. 1(i) shows the battery equivalent circuit during the discharge phase. R_{ex} is the external resistor. Fig. 1(ii) shows the battery equivalent circuit in the rest period that follows the discharge phase.

Fig. 2(i) shows the battery circuit during the charge phase. V_g is the charging voltage. The charge phase is followed by a rest period represented by Fig. 2(ii). The same battery model applies in the charge phase as in the discharge one but now with different values for the components in the parallel circuit. The capacitor value is C_2 for both the charge and the subsequent rest period, while R_3 and R_4 are the resistors in parallel with the capacitor in the charge and rest periods, respectively. The series resistor R stays the same as in the discharge–rest case. Since $V_g > V_{oc}$ the voltage source V_g acts as a generator. The current $i(t)$ flows into terminal a and ultimately into the positive terminal of V_{oc} as a

* Tel.: +1 610 758 4082; fax: +1 610 758 6279.
E-mail address: khn0@lehigh.edu

0378-7753/$ – see front matter © 2011 Elsevier B.V. All rights reserved.
doi:10.1016/j.jpowsour.2011.04.002

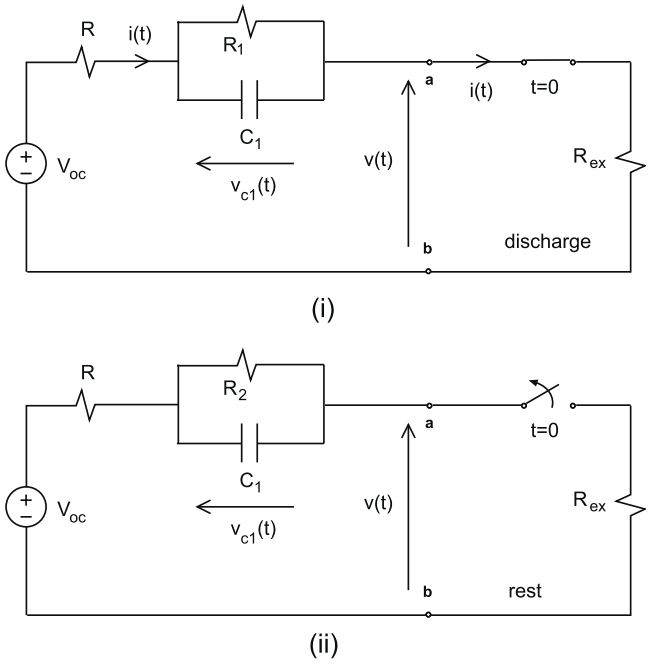

Fig. 1. The circuit for (i) the discharge period and (ii) the subsequent rest phase of the battery. $v(t)$ is the battery voltage and R_{ex} is the external load resistor. V_{oc} is the open circuit voltage of the battery. R is the series resistance in the battery equivalent circuit.

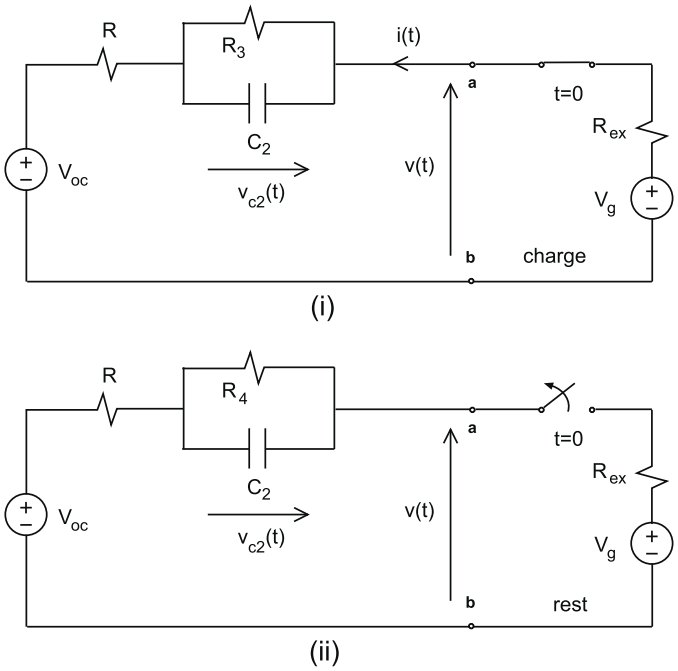

Fig. 2. The equivalent circuit for the battery in (i) the charging phase followed by (ii) the resting period. V_g is the external charging voltage. $V_g > V_{oc}$.

charging current to the battery. The source V_{oc} now acts as the energy absorber.

Transients are involved during the charging and discharging of batteries. Abrupt changes are recorded in the voltage across the terminals of the battery as the switch is closed or opened at the start of these transients. These boundary value changes in voltage as well as voltage levels in the intervening transients are used here to calculate circuit parameters. The temporal variation of the voltage across the battery terminals during the discharge–rest–charge–rest sequence appears in Fig. 3. The equations for the variation in the battery voltage $v(t)$ during the discharge–rest–charge–rest sequence were derived earlier [12,13]. These equations correspond to the voltage levels V_1 to V_7 that are shown in Fig. 3 and are relevant to the measurement technique used here. The equations that were used to calculate the equivalent circuit parameters of the NiMH battery are

$$R = R_{ex}\left(\frac{V_{oc}}{V_2} - 1\right) \tag{1}$$

$$R_1 = R\left(\frac{V_{oc}}{V_4 - V_3} - 1\right) - R_{ex} \tag{2}$$

$$R_2 = \frac{R_1 V_{oc}}{(R + R_1 + R_{ex})C_1(dv/dt)_{r1}} \tag{3}$$

$$C_1 = -\frac{R_{ex}V_{oc}}{(R + R_{ex})^2(dv/dt)_d} \tag{4}$$

$$R_3 = R\left(\frac{V_g - V_{oc}}{V_6 - V_7} - 1\right) - R_{ex} \tag{5}$$

$$R_4 = -\frac{R_3(V_g - V_{oc})}{(R + R_3 + R_{ex})C_2(dv/dt)_{r2}} \tag{6}$$

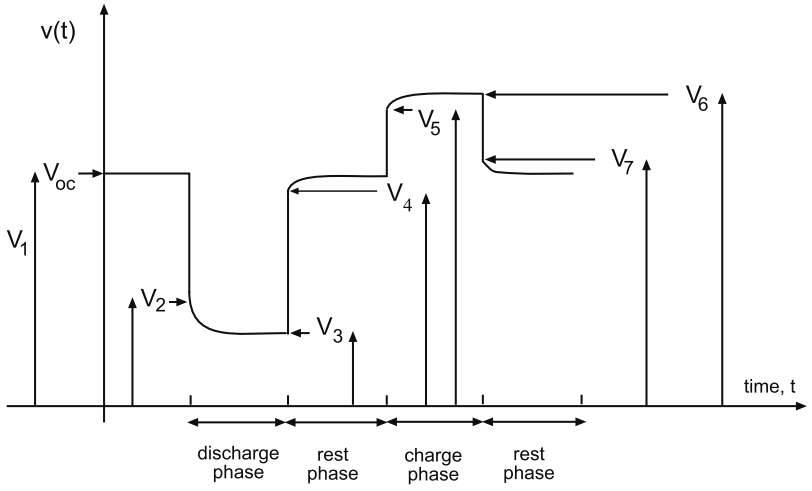

Fig. 3. The battery terminal voltage $v(t)$ as a function of time during the discharge and rest phases, followed by the charge and rest phases showing the voltage levels V_1 to V_7.

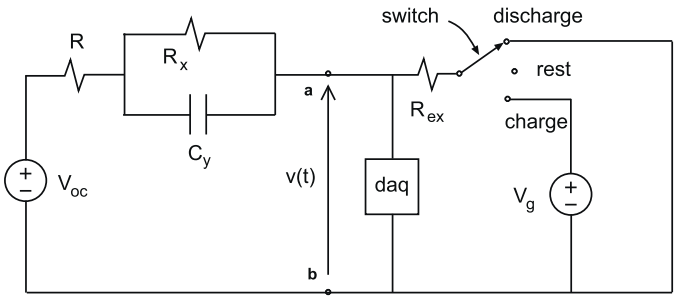

Fig. 4. The circuit used for measuring the temporal variation of the battery voltage during the discharge–rest–charge–rest phases.

$$C_2 = \frac{R_{ex}(V_g - V_{oc})}{(R + R_{ex})^2 (dv/dt)_c} \quad (7)$$

where the respective gradients at the start of the discharge phase and at the start of the subsequent rest period are $(dv/dt)_d$ and $(dv/dt)_{r1}$, respectively, while the respective gradients at the start of the charge phase and at the start of the subsequent rest period are given by $(dv/dt)_c$ and $(dv/dt)_{r2}$.

3. Experimental

NiMH batteries rated at 1.2 V, and a 10 h capacity of 2300 mAh were examined. The discharge–rest–charge–rest curve of a fully charged battery was first obtained. The battery was then discharged to 70% SOC and then to 40% SOC and the discharge–rest–charge–rest curve at each SOC was recorded. Each curve was a plot of the battery voltage $v(t)$ as a function of time and was recorded with the battery at room temperature. Fig. 4 shows the circuit used for measuring the discharge–rest–charge–rest curve. A single pole double throw switch with center off was used to switch between phases and the resulting temporal variation in the battery voltage was recorded by connecting the data acquisition (daq) probe between terminals *a* and *b*. Fig. 5 shows the discharge–rest–charge–rest curve of a battery at 100% SOC.

Table 1
Component values of the equivalent circuit of three NiMH batteries of equal capacity at states of charge of 40%, 70% and 100%.

SOC	40%	70%	100%
(i)			
R	0.11 Ω	0.11 Ω	0.10 Ω
R_1	0.01 Ω	0.01 Ω	0.01 Ω
R_2	0.01 Ω	0.01 Ω	0.01 Ω
C_1	21.10 F	19.41 F	13.76 F
R_3	0.01 Ω	0.01 Ω	0.01 Ω
R_4	0.03 Ω	0.02 Ω	0.02 Ω
C_2	4.27 F	5.03 F	7.85 F
(ii)			
R	0.05 Ω	0.05 Ω	0.05 Ω
R_1	0.01 Ω	0.01 Ω	0.01 Ω
R_2	0.01 Ω	0.01 Ω	0.01 Ω
C_1	20.25 F	18.06 F	12.92 F
R_3	0.01 Ω	0.01 Ω	0.01 Ω
R_4	0.02 Ω	0.02 Ω	0.02 Ω
C_2	4.14 F	4.82 F	7.24 F
(iii)			
R	0.16 Ω	0.16 Ω	0.14 Ω
R_1	0.03 Ω	0.03 Ω	0.02 Ω
R_2	0.03 Ω	0.03 Ω	0.03 Ω
C_1	20.07 F	18.32 F	12.36 F
R_3	0.03 Ω	0.03 Ω	0.03 Ω
R_4	0.04 Ω	0.04 Ω	0.02 Ω
C_2	3.80 F	4.94 F	6.96 F

The charging voltage V_g during the charge phase was 1.6441 V for all experiments. The external load resistor R_{ex} was 10 Ω. The open circuit battery voltage V_{oc} was 1.2950 V, 1.3875 V and 1.4038 V at 40%, 70% and 100% SOC, respectively.

The battery displayed large abrupt voltage changes at the beginning of each phase in its discharge–rest–charge–rest curve. These changes in $v(t)$ were then followed by transients of short duration

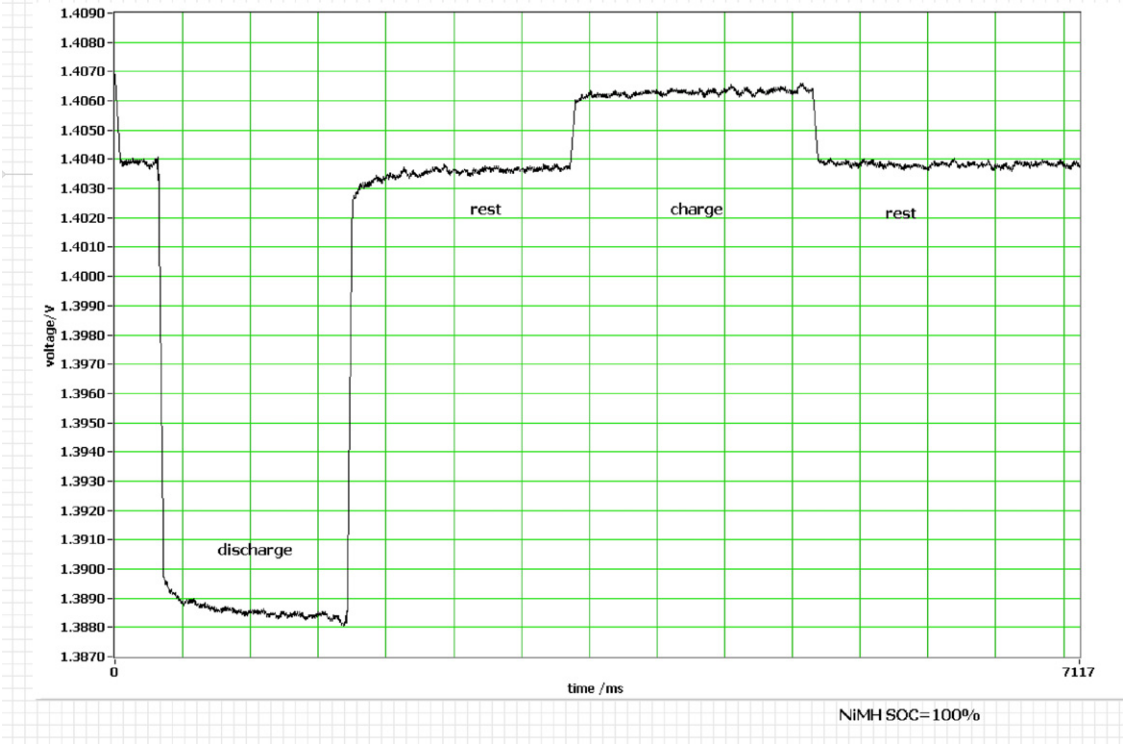

Fig. 5. The temporal variation of the battery voltage $v(t)$ in the discharge–rest–charge–rest characteristics of a NiMH battery at a state of charge of 100%.

where the battery voltage recovered to a steady state value within seconds.

Circuit components could be calculated to within ±0.02. The component values of the equivalent circuit of the battery are given in Table 1. All resistors, R, R_1, R_2, R_3 and R_4 are approximately constant as the SOC decreases from 100% to 40%. Also, C_1 increases while C_2 decreases as the SOC decreases. The same trends were seen in the other NiCad batteries with the same rating that were examined by the author.

The change in capacitance with changes in SOC provides a useful means of battery evaluation for NiMH batteries. For example, for the battery with parameters shown in Table 1(i), the changes in capacitance are from 13.76 F to 21.10 F for C_1 and from 7.85 F to 4.27 F for C_2 as the SOC decreases from 100% to 40%. Therefore, the value of the capacitor in the parallel RC circuit of the battery equivalent can be used as an indicator of the battery SOC.

4. Conclusions

Equations that describe the voltage variations with time of rechargeable batteries during charging and discharging, and in the boundary regions between these phases, were used to determine the component values of the equivalent circuit of nickel–metal hydride batteries under different states of charge. The results show that the resistances in the equivalent circuit are approximately constant with variations in the state of charge. For the discharge and charge phases the capacitor value increased and decreased, respectively, as the SOC decreased. The value of the capacitor in the parallel resistor–capacitor circuit is an indicator of the battery SOC.

References

[1] I. Damlund, 17th International Telecommunications Energy Conference, 1995, pp. 828–833, doi:10.1109/INTLEC.1995.499055.
[2] K. Bundy, M. Karlsson, G. Lindbergh, A. Lundqvist, Journal of Power Sources 72 (2) (1998) 118–125.
[3] K.S. Ng, Y.F. Huang, C.S. Moo, Y.C. Hsieh, 31st Telecommunications Energy Conference, 2009, pp. 1–5, doi:10:1109/INTLEC.2009.5351796.
[4] C.S. Moo, K.S. Ng, Y.P. Chen, Y.C. Hsieh, IEEE Power Conversion Conference, Nagoya, 2007, pp. 758–762, doi:10.1109/PCCON.2007.373052.
[5] H. Bode, Lead Acid Batteries, John Wiley, New York, 1977.
[6] M.A. Dasoyan, I.A. Aguf, Current Theory of Lead Acid Batteries, Technicopy, Ltd., England, 1979.
[7] Z.M. Salameh, M.A. Casacca, W.A. Lynch, IEEE Transactions on Energy Conversion 7 (1) (1992) 93–98.
[8] M.A. Casacca, Z.M. Salameh, IEEE Transactions on Energy Conversion 7 (3) (1992) 442–446.
[9] H.L. Chan, D. Sutanto, IEEE Power Engineering Society Winter Meeting vol.1, Singapore, 2000, pp. 470–475.
[10] W.A Lynch, Z.M. Salameh, IEEE Power Engineering Soc. Meeting, Montréal, 2006 (Paper no. 06 GM1201).
[11] S.R. Nelatury, P. Singh, Journal of Power Sources 112 (2002) 621–625.
[12] K.H. Norian, Journal of Power Sources 196 (2011) 2360–2363.
[13] K.H. Norian, Journal of Power Sources 196 (2011) 5205–5208.